

Downregulation of Androgen Receptor Transcription by Promoter G-Quadruplex Stabilization as a Potential Alternative Treatment for Castrate-Resistant Prostate Cancer

Tom Mitchell,^{*,†} Antonio Ramos-Montoya,[†] Marco Di Antonio,[‡] Pierre Murat,[‡] Stephan Ohnmacht,[§] Marialuisa Micco,[§] Sarah Jurmeister,[†] Lee Fryer,[†] Shankar Balasubramanian,^{†,‡} Stephen Neidle,[§] and David E. Neal[†]

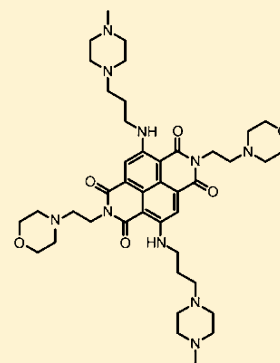
[†]CRUK Cambridge Research Institute, Li Ka Shing Centre, Robinson Way, Cambridge CB2 0RE, U.K.

[‡]Department of Chemistry, University of Cambridge, Lensfield Road, Cambridge CB2 1EW, U.K.

[§]UCL School of Pharmacy, University College London, London WC1N 1AX, U.K.

S Supporting Information

ABSTRACT: Androgen receptor (AR) signaling remains an important regulatory pathway in castrate-resistant prostate cancer, and its transcriptional downregulation could provide a new line of therapy. A number of small-molecule ligands have previously demonstrated the ability to stabilize G-quadruplex structures and affect gene transcription for those genes whose promoters contain a quadruplex-forming sequence. Herein, we report the probable formation of new G-quadruplex structure present in the AR promoter in a transcriptionally important location. NMR spectroscopy, circular dichroism, UV spectroscopy, and UV thermal melting experiments for this sequence are consistent with G-quadruplex formation. Fluorescence resonance energy transfer (FRET) melting studies have identified a novel compound, MM45, which appears to stabilize this G-quadruplex at submicromolar concentrations. The effects of MM45 have been investigated in prostate cancer cell lines where it has been shown to inhibit cell growth. A reporter assay intended to isolate the effect of MM45 on the G-quadruplex sequence showed dose-dependent transcriptional repression only when the AR promoter G-quadruplex sequence is present. Dose-dependent transcriptional repression of the AR by MM45 has been demonstrated at both a protein and mRNA level. This proof of concept study paves the route toward a potential alternative treatment pathway in castrate-resistant prostate cancer.



The androgen receptor (AR) plays a key role in prostatic growth in both benign and malignant disease.¹ As such, androgen deprivation therapy represents the main initial treatment for advanced prostate cancer.¹ Unfortunately, tumors will ultimately progress despite androgen deprivation and are then termed castrate-resistant.¹ In most cases of castrate-resistant prostate cancer (CRPC), AR signaling persists despite androgen blockage. Multiple mechanisms have been attributed to the emergence of CRPC and include amplification of AR gene, gain of function mutation of the AR, local intracellular androgen synthesis, and AR splice variants that display constitutive activity in the absence of ligand binding.¹ As no significant somatic mutations have been detected in the AR gene promoter,² repression of AR transcription could consistently evade many of the currently documented mechanisms that are attributed to the emergence of CRPC.

Other specific therapies targeting the AR have recently shown efficacy in clinical trials in both direct blockade of the AR ligand-binding domain (MDV-3100³) and further reducing androgenic steroid production (Abiraterone acetate⁴). Inevitably, resistance also develops to these therapies, often through maintenance of AR signaling by the evading mechanisms described above.⁵

Most cases of CRPC are associated with an increase in AR protein production.⁶ The increase in the AR has been shown to be both necessary and sufficient to convert prostate cancer growth from a hormone-sensitive to a hormone-refractory stage in prostate cancer cell lines.⁷ Furthermore, knockdown of the androgen receptor has been shown to cause growth inhibition and regression of castrate-resistant tumors in xenografts.⁸

Transcriptional repression of AR signaling is not a novel treatment approach. Epigenetic modifications, in particular histone deacetylase inhibitors, have been shown to decrease AR protein levels in both castration-sensitive and -refractory prostate cancer by blocking AR mRNA synthesis.⁹ This has been applied clinically, though phase II clinical trials revealed only minimal antitumor activity with romidepsin, a histone deacetylase inhibitor.¹⁰

Downregulation of AR transcription therefore offers a potentially favorable treatment pathway for CRPC and by acting upstream can potentially consistently circumvent the mechanisms causing castrate resistance.

Received: October 3, 2012

Revised: January 28, 2013

Published: January 30, 2013



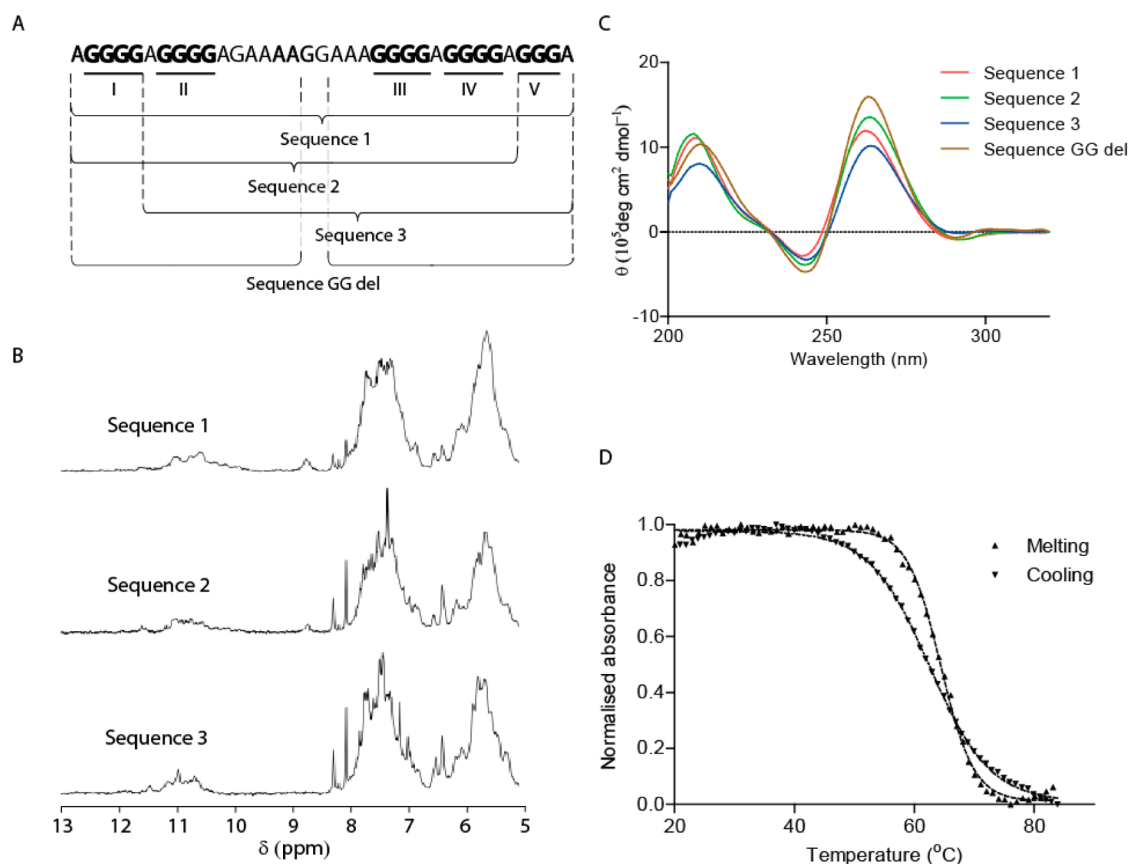


Figure 1. Biophysical characterization of the androgen receptor promoter G-quadruplex. (A) Nucleotide sequence from androgen receptor promoter –116 base pairs from its transcription start site can form many possible G-quadruplex conformations. The three sequences that are further characterized are annotated. (B) ^1H NMR spectra of G-quadruplex formation for the three oligonucleotide sequences at 298 K in buffer containing 70 mM K^+ . (C) Circular dichroism spectra for the three sequences indicating parallel quadruplex conformation in a 100 mM K^+ buffer. (D) UV spectroscopic melting curves for sequence 3 in a 100 mM K^+ buffer.

G-quadruplexes are noncanonical higher-order nucleic acid structures that form from repeats of short G-tracts, with the underlying structural motif being the planar arrangement of four strands of guanine bases stacked upon one another in G-rich DNA and RNA tracts (the G-quartet).¹¹ The exploitation of their occurrence in a number of gene promoters and their potential as targets for an anticancer strategy has been recently developed.¹² G-quadruplex structures possess highly variable loop and groove structural features on their surfaces that can provide favorable binding of small-molecules that can stabilize (or sometimes destabilize) the G-quadruplex unit. When occurring in gene promoters, a stabilized quadruplex unit can downregulate gene expression, possibly by blocking the transcriptional machinery or by inhibiting transcription factor binding.¹²

G-quadruplex structures have been described and characterized in a number of oncogenic promoter regions including those of the c-MYC,¹³ c-KIT,¹⁴ and KRAS¹⁵ genes. The clinical potential of G-quadruplex binding with small molecules in downregulating gene transcription has been demonstrated through phase II clinical trials.¹⁶ In particular, naphthalene diimide scaffolds have shown promise to tightly and selectively recognize G-quadruplex structures.^{17,18} With >40% of gene promoters containing putative G-quadruplex forming sites,¹⁹ global genomic effects of G-quadruplex binding ligands still need to be fully understood.²⁰

We found a putative G-quadruplex forming sequence in the minimal AR promoter and is positioned 116 bp upstream of the AR transcription start site. The sequence is shown in Figure 1A.

This location is 36 bp upstream of a confirmed Sp1 binding site that plays a central role in AR transcription initiation.²¹ A mutation/deletion analysis of the AR promoter has demonstrated the importance of the putative G-quadruplex forming sequence where deletion of the –276/–74 bp sequence decreased AR gene transcription by a factor over 4-fold, possibly by co-operative enhancement with an oligonucleotide sequence downstream of the transcription start site.²²

Herein, we describe biophysical characterization of this new putative G-quadruplex sequence in the AR promoter by methods previously well documented in the literature.^{23–26} We use a FRET screen to identify small molecules that effectively bind to this sequence. The hit obtained by this method has been compared to a compound that is less effective at FRET determine quadruplex binding by growth assays in a range of prostate cancer cell lines. The potency of this ligand in the regulation of AR expression has been assessed through the use of a reporter assay and in quantifying AR protein and mRNA levels.

METHODS

Biophysical Oligonucleotides. HPLC grade oligonucleotides for UV, CD, and NMR spectroscopy are shown in Table S1.

For FRET experiments, HPLC grade 5'-FAM (5'-carboxyfluorescein) and 3'-TAMRA (3'-6-carboxytetramethylrhodamine) labeled oligonucleotides for sequence 3, a telomeric DNA control sequence, and a duplex control sequence are also shown in Table S1.

UV Spectroscopy. Ultraviolet (UV) spectroscopic melting curves were collected using a Varian Cary 400 Scan UV-vis spectrophotometer by following absorbance at 295 nm. Oligonucleotides solutions were prepared at a final concentration of 4 μ M in 10 mM lithium cacodylate (pH 7.2) containing 1 mM EDTA and 100 mM KCl. The samples were annealed by heating to 95 °C for 10 min and then slowly cooled to 4 °C. Samples were transferred to a 1 cm path-length quartz cuvette, covered with a layer of mineral oil, placed in the spectrophotometer, and equilibrated at 5 °C for 10 min. Samples were then heated to 95 °C and cooled back to 5 °C at a rate of 1 °C/min, with data collection every 1 °C during both melting and cooling. T_m values were obtained from the minimal of the first derivative of the melting curve.

CD Spectroscopy. Circular dichroism (CD) experiments were conducted on a Chirascan spectropolarimeter using a quartz cuvette with an optical path length of 1 mm. Oligonucleotide solutions were prepared at a final concentration of 10 μ M in 10 mM lithium cacodylate (pH 7.2) containing 1 mM of EDTA and either 100 mM of KCl, NaCl, or LiCl. The samples were annealed by being heated at 95 °C for 10 min and slowly cooled to 4 °C. Scans were performed over the range of 200–320 nm at 25 °C. Each trace is the result of the average of three scans taken with a step size of 1 nm, a time per point of 1 s, and a bandwidth of 0.5 nm. A blank sample containing only buffer was recorded under the same conditions and subtracted from the oligonucleotides spectra. The data were zero-corrected at 320 nm. CD melting was performed for all three sequences in the same buffer. The sequences were heated from 25 to 95 °C at a rate of 1 °C/min at a wavelength of 260 nm.

NMR Spectroscopy. ^1H nuclear magnetic resonance (NMR) spectra were recorded at 298 K using a 500 MHz Bruker Avance 500 TCI spectrometer equipped with a cryogenic TCI ATM probe. Water suppression was achieved using excitation sculpting. The oligonucleotides were annealed in a 10 mM PBS buffer (pH 7.0) supplemented with 70 mM KCl and 10% D_2O at a final concentration of 0.1 mM. The samples were annealed by being heated at 95 °C for 10 min and slowly cooled to room temperature.

FRET. The FRET probe sequences were diluted to 400 nM in a 60 mM potassium cacodylate buffer (pH 7.4) and then annealed by heating to 95 °C for 10 min, followed by cooling to room temperature in the heating block (3–3.5 h). The synthesis of the naphthalene diimide compound MM45 will be described elsewhere. Purification was achieved using C18 reverse-phase semiprep HPLC. The compounds were stored as a 1 mM stock solution in 10% DMSO/90% 1 mmol HCl; final solutions (at 2 \times concentration) were prepared using 60 mM potassium cacodylate buffer (pH 7.4). The 96-well plates were prepared by aliquoting 50 μ L of the annealed DNA into each well, followed by 50 μ L of the compound solutions. Measurements were made on a DNA Opticon (MJ Research) with excitation at 450–495 nm and detection at 515–545 nm. Fluorescence readings were taken at intervals of 0.5 °C in the range 30–100 °C, with a constant temperature being maintained for 30 s prior to each reading to ensure a stable value.

Final analysis of the data was carried out using a script written in the program Origin 7.0 (OriginLab Corp., Northampton, MA). The advanced curve-fitting function in Origin 7.0 was used for calculation of ΔT_m values (± 0.1 °C).

Cell Culture. LNCaP, PC3, DU145, and PNT1a cells were obtained from ATCC, C4-2, and C4-2b cells from MD Anderson Cancer Centre, Houston, TX. Prostate cancer cell lines were all cultured in RPMI media with L-glutamine and supplemented with 10% fetal calf serum. All cells were cultured at 37 °C and 5% CO_2 .

Cell Proliferation Assay. Apparent half-maximal inhibitor concentration (IC_{50}) values of growth inhibition were determined using the MTS cell proliferation assay CellTiter 96 AQueous from Promega (Madison, WI). Cells were seeded in 96-well plates at 4000 cells/well on day 0 in 90 μ L of media. MM45 was added in serial dilutions (for final concentrations from 100 to 0 μ M in 11 dilutions of 2.5 \times) in 10 μ L of media. Cell viability was measured at 72 h using the manufacturer's protocol. Measurements were taken 1 h after the addition of the assay. All measurements were made in octuplets. Final analysis was carried out using GraphPad Prism 5 (San Diego, CA).

Viability Assay by Trypan Blue Dye Exclusion. Cell viability was measured using the trypan blue dye exclusion method with a Vi-Cell series cell analyzer. LNCaP cells were seeded at 0.5×10^6 cells per well in 1.8 mL of media in a 6-well plate on day 0. The following day compound MM45 was added in 0.2 mL aliquots to the cells to give final concentrations of 4, 2, 0.4, and 0 μ M. Cells and their media were harvested at 6, 12, 24, or 48 and 72 h by spinning down incubated media and trypsinised cells before suspending in 500 μ L of PBS. Cells were then added to the analyzer according to manufacturer's instructions. All measurements were made in triplicate.

Luciferase Reporter Assay. The Luc2CP gene was excised from the pGL4.16 Vector (Promega) and inserted into a pCSC-SP-PW vector (Addgene). The PGK-Puromycin resistance cassette was inserted afterward to generate the pCSC-Luc2CP-Puro lentiviral vector. Two fragments of the AR promoter, generated by PCR (primers detailed in Table S1) from LNCaP genomic DNA, were inserted into the vector. Both fragments contained the same promoter region, with the only difference of either containing (221 bp) or not (156 bp) the G-quadruplex sequence.

HEK293TLA cells were transfected by calcium phosphate. Media was changed after 24 h and fresh media applied. After a further 24 h viral supernatant was filtered (22 μ m pore size, Millipore, Billerica, MA), mixed with fresh media, and used to infect the cells.

The LNCaP reporter cell lines were grown in RPMI with 10% FBS + puromycin 2 μ g/mL. HEK293TLA (Open Biosystems, Lafayette, CO) cells were maintained in Dulbecco's modified Eagle's medium (DMEM) with 10% FBS, (Invitrogen). Cells were grown at 37 °C in an atmosphere containing 5% CO_2 .

Luminescence was measured using the Xenogen IVIS 200 optical imaging system. Luminescent measurements were analyzed using Xenogen Imaging Analysis software "Living Image 3.0" (Caliper Life Sciences) and plotted as photons/s for analysis.

To investigate the effect of compound MM45 on luciferase activity, cells were seeded at 45×10^3 cells per well in 90 μ L of medium in 96-well plates on day 0. On day 1, MM45 was added to each well in 10 μ L of medium to make up the average

well concentration as indicated. Six replicates for each condition and each cell line were used. At 6 h, 20 μL of luciferin was added to each well (final 150 ng/mL) and the plate imaged as above. Luminescence of each well was normalized for cell number by MTS assay immediately after measuring luciferase expression. Experiments were independently repeated three times.

Western Blots. LNCaP cells were seeded on day 0 at 0.5×10^6 cells per well in 6-well plates in 1.8 mL of RPMI media supplemented with 10% fetal bovine serum. On day 1 MM45 was added in 0.2 mL of media to make up the desired final concentrations of 4, 2, 0.4, and 0 μM . 24 h after drug addition, cells were lifted into a RIPA buffer, sonicated, and denatured. Samples were run together for resolution by SDS polyacrylamide gel electrophoresis, transferred to nitrocellulose, and blotted with appropriate mouse monoclonal antibody (AR; AR441 and β -actin; AC-15). Triplicate samples were analyzed. Blot quantification was performed using ImageQuant TL 1 D gel analysis software.

PCR. LNCaP cells were seeded on day 0 at 1.5×10^6 cells per well in 6 cm plates in 2.7 mL of RPMI media supplemented with 10% fetal bovine serum. On day 1, MM45 was added in 0.3 mL of media to make up the desired final concentration. Gene expression was measured by Sybr green in 384-well plates run in an Applied Biosystems 7900HT fast real-time PCR system. Primers are shown in Table S1. Absolute quantification of RNA levels was determined using standard curves. Relative expression was calculated according to vehicle and housekeeping genes TBP and SDH. Sample quadruplicates and technical triplicates were run.

RESULTS

Biophysical Characterization of the Androgen Receptor G-Quadruplex. The full-length oligonucleotide sequence containing the G-quadruplex structure contains five runs of consecutive guanine bases. As only four guanine tracts typically containing three consecutive guanine bases are required to form a quadruplex, we assumed that the sequence could have led to a polymorphic structure. To determine which tracts form the dominant structure, the full oligonucleotide tract studied has been split into two smaller fragment and subjected to biophysical characterization (Figure 1A). The full-length sequence was also analyzed with the two central guanine bases deleted to determine whether they contribute to the structural integrity of the G-quadruplex.

NMR spectroscopy confirmed spectra consistent with quadruplex formation for all three fragments at 298 K in a 70 mM K^+ buffer (Figure 1B). The increase in signal between 10 and 12 ppm is consistent with emission from imino protons bound by Hoogsteen H-bonds and infers quadruplex formation in all sequences.²⁴ The absence of individual discrete peaks in the 10–12 ppm range is consistent with conformational heterogeneity, with sequence 3 appearing the least polymorphic.

Circular dichroism revealed curves typical of parallel or group I quadruplex topology for all sequences including with the central two guanine bases deleted (Figure 1C).²³ Similar results were seen on replacing the potassium cationic buffer with either sodium or lithium cations (Figure S1). The fact that these sequences are still folding into G-quadruplex structures in Li^+ buffers suggests high propensity to generate stable G-quadruplexes in a cation-independent fashion. CD melting

recorded at 245 nm (25–92.5 $^{\circ}\text{C}$) further demonstrated the high stability of the AR G-quadruplex (Figure S2).

As sequence 3 showed the least heterogeneity on NMR spectroscopy, this was investigated further with UV denaturation and also for FRET melting studies. Typical quadruplex melting and cooling curves were revealed with melting and cooling temperatures of 65.7 and 62.5 $^{\circ}\text{C}$, respectively (Figure 1D).

FRET Melting Determines Stabilization of the Androgen Receptor G-Quadruplex by the Compound MM45. FRET melting was used as a screen for compounds that bound with greatest affinity to the dual-labeled (5'-FAM and 3'-TAMRA) sequence 3. Seven naphthalene diimide compounds were screened, and their ability to stabilize duplex, telomeric, and sequence 3 quadruplex structures was determined by quantifying the change in melting temperature (ΔT_m) values. MM45 (structure and compositional nomenclature in Figure 2A) had the greatest ability to stabilize the AR

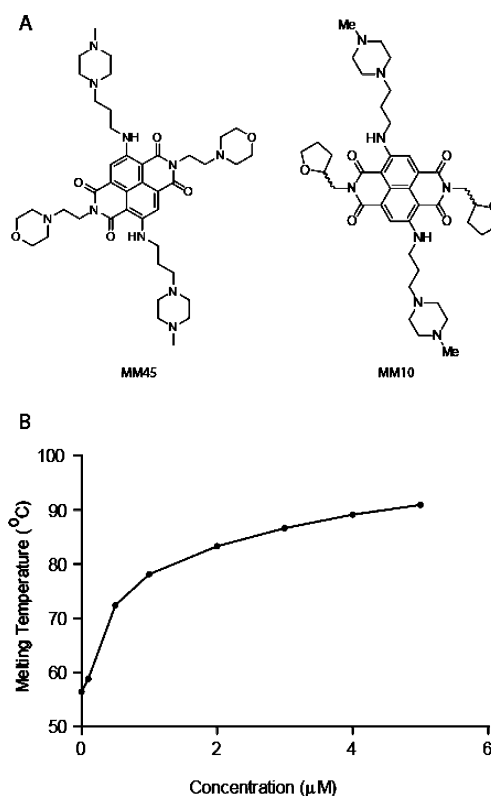


Figure 2. Stabilization of the androgen receptor G-quadruplex by MM45. (A) Molecular structure of MM45 (4,9-bis((3-(4-methylpiperazin-1-yl)propyl)amino)-2,7-bis(2-morpholinoethyl)benzo[1,3,8]phenanthroline-1,3,6,8-tetraone) and MM10. (B) Melting temperature for sequence 3 with increasing dose of MM45. The oligonucleotides were dual-labeled with donor FAM and acceptor TAMRA fluorophores and intensity measured with increasing concentration of the G-quadruplex stabilization ligand MM45.

promoter sequence 3 with a ΔT_m of 14.9 ± 0.4 $^{\circ}\text{C}$ at a MM45 concentration of 0.5 μM . This compares to a ΔT_m of 25.8 ± 0.06 $^{\circ}\text{C}$ to telomeric DNA and ΔT_m of 0.2 ± 0.03 $^{\circ}\text{C}$ to duplex DNA. The melting curve of sequence 3 with increasing concentration of MM45 is shown in Figure 2B. MM10 was used as a negative control in the cellular studies as it was the least active naphthalene diimide compound. This gave a ΔT_m of 7.58 ± 0.07 $^{\circ}\text{C}$ at a concentration of 0.5 μM .

Inhibition of Growth of Prostate Cancer Cell Lines by MM45. Concentrations of MM45 and MM10 for growth inhibition across five prostate cancer cell lines and one epithelial cell line derived from normal prostatic epithelium (PNT1a) were calculated by MTS assay at 72 h and are shown in Figure 3A. C4-2 and C4-2b cell lines are derived from the

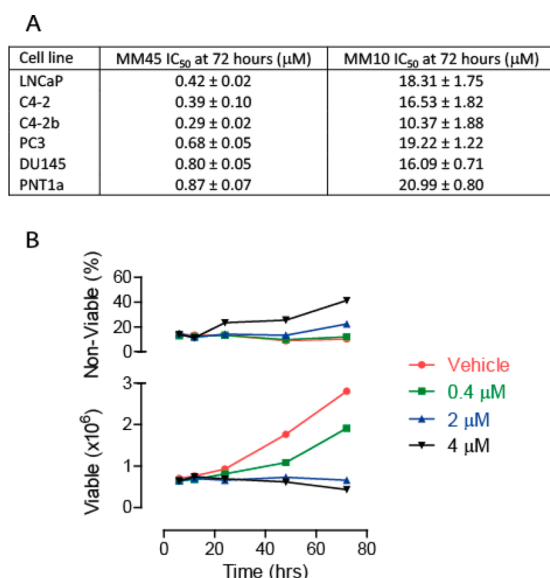


Figure 3. Inhibition of growth of prostate cancer cell lines by MM45. (A) MTS derived IC₅₀ data at 72 h for MM45 and MM10 in six different prostate cell lines. Values ± SD are given. (B) Inhibition of growth of LNCaP cells by MM45 as quantified by trypan blue exclusion. Cell counts were performed 6, 16, 24, 48, and 72 h after addition of MM45 at the final concentrations indicated.

metastatic LNCaP and all express the AR. C4-2 and C4-2b cell lines have reduced androgen sensitivity compared to LNCaP but do maintain AR transcriptional activity.²⁷ The PC3 and DU145 cell lines both do not express AR and as such are relatively insensitive to inhibition of AR transcription.²⁸ The MTS data show the cell lines dependent on AR transcriptional activity are more sensitive to MM45 than the AR negative cell lines by a factor of 2 ($p < 0.05$ by one-way ANOVA analysis). This may be accounted for by differences in cellular uptake of MM45. However, there is no such statistical difference between IC₅₀ values of AR positive and negative cell lines with MM10 (p

> 0.05 by one-way ANOVA analysis). The negative control, MM10, was far less potent at inhibiting cell growth than MM45.

Effects of MM45 on cell growth and death in LNCaP cells were further investigated by a trypan blue exclusion study (Figure 3B). Cell growth and cell death were measured 6, 12, 24, 48, and 72 h after addition of vehicle control, 0.4, 2, or 4 μM final concentration of MM45 (approximately equivalent to the 72 h IC₅₀, 5xIC₅₀, and 10xIC₅₀ for LNCaP cells). There is a temporal dose-dependent inhibition of cellular growth and decrease in cellular viability ($p > 0.05$, two-way ANOVA).

Interaction of MM45 with the G-Quadruplex Sequence in the Androgen Core Promoter by Reporter Assay. To determine whether MM45 could stabilize the AR core promoter quadruplex sequence and affect transcription in cells, two stable LNCaP cell lines were cloned with the AR core promoter attached to a luciferase reporter assay. The first, “G4” cell line included the G-quadruplex forming sequence, beginning 125 bp upstream of the transcription start site and ending 126 bp downstream of the transcription start site. The second “control” had the quadruplex sequence deleted but maintained the Sp1 binding site and began 58 bp upstream of the transcription start site (Figure 4A). Expression was roughly twice as intense for the “G4” cell line in comparison with “control”, a finding in line with the premise that this region is transcriptionally important.

Luciferase expression was quantified in both cell lines 6 h after varying concentrations of MM45 were added. Luciferase activity relative to vehicle is shown in Figure 4B. The “G4” cell line exhibits a dose-dependent inhibition of luciferase activity, whereas the only significant decrease in luciferase activity in the control cell line occurs at the maximal concentration or 4 μM. Two-way ANOVA analysis reveals a dose-dependent statistically significant difference between the G4 and control lines ($p < 0.0001$).

Downregulation of Androgen Receptor Transcription by MM45. Protein levels were measured for AR and the housekeeping gene actin in LNCaP cells 24 h after MM45 drug challenge at final concentrations of 0.4, 2, and 4 μM (Figure 5A). AR protein levels relative to actin were also quantified where a 4-fold reduction was seen at the maximum MM45 dosage. The dose-dependent decrease in AR levels with MM45 concentration is confirmed by statistical analysis ($p = 0.0012$, two-way ANOVA).

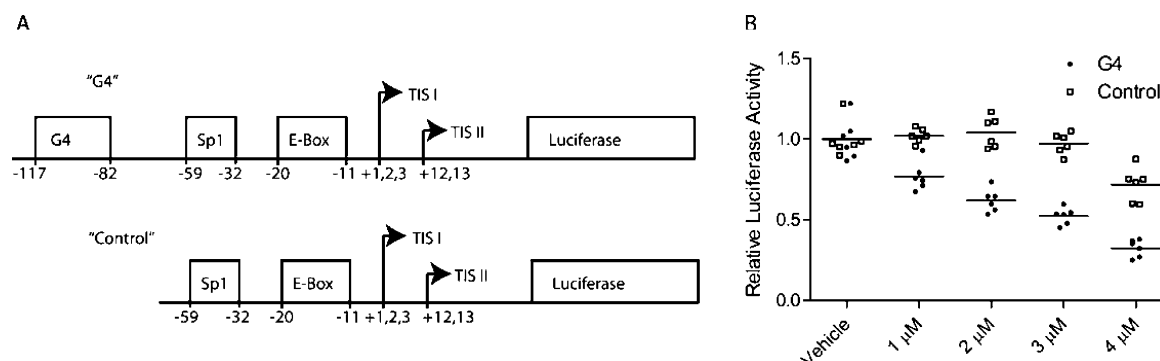


Figure 4. Interaction of MM45 with the androgen receptor core promoter by reporter assay. (A) Schematic representation of the two, stable luciferase labeled reporter assays. Both contain the core androgen receptor promoter, “G4” contains the G-quadruplex sequence, but the second “control” was shortened to exclude the G-quadruplex forming oligonucleotides. (B) Dose-dependent relative luciferase activity of the cell line containing the G-quadruplex sequence and the control cell line 6 h after addition of the indicated final drug concentrations.

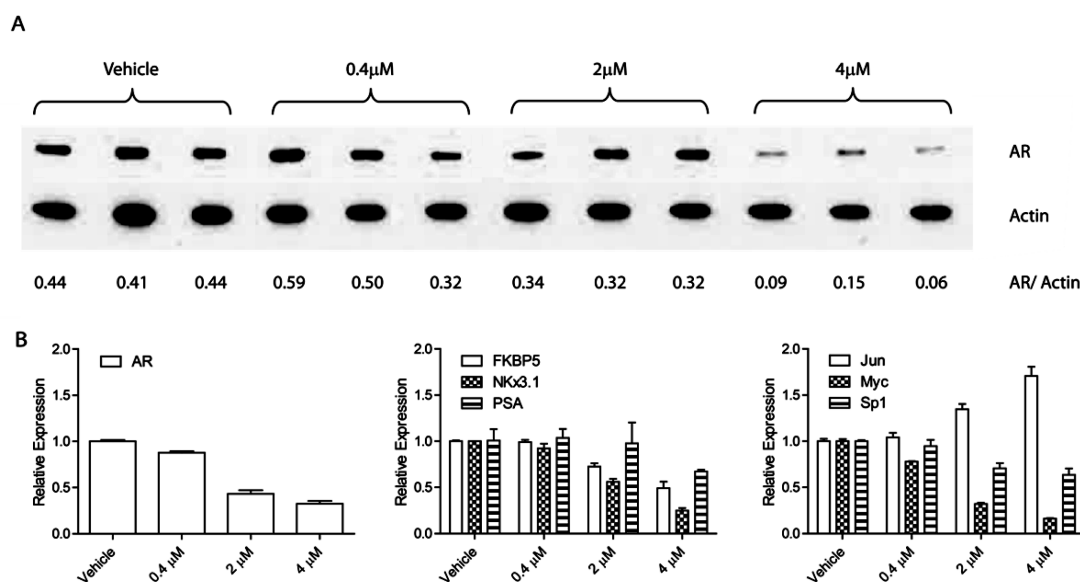


Figure 5. Downregulation of androgen receptor transcription. (A) Paired Western blots for the androgen receptor and housekeeping protein actin at 24 h after addition of the indicated dose of MM45. Relative protein levels of the androgen receptor compared to actin have been quantified are shown below each sample. (B) RT qPCR at 6 h after addition of indicated final concentration of MM45 for the androgen receptor, androgen-responsive genes FKBP5, NKX3.1, and PSA, and androgen receptor upstream transcription factors Jun, Myc, and Sp1. All levels are relative to the housekeeping gene TBP.

Transcriptional levels of the AR, the androgen response genes FKBP5, NKX3.1, and PSA, and upstream AR gene transcription factors Jun, Myc, and Sp1 were quantified 6 h after challenge with MM45 at 0.4, 2, and 4 μ M. Levels were calculated relative to either housekeeping gene SDH or TBP and are shown relative to TBP (Figure 5B). Equivalent results were seen relative to SDH. AR mRNA levels are inversely correlated with MM45 concentration ($p < 0.0001$ one-way ANOVA). AR-responsive genes show a similar correlation, indicating that functional AR activity has been inhibited. AR transcription factors were also investigated. The relative expression of Jun increased, whereas Myc and Sp1 decreased with MM45 concentration.

DISCUSSION

In this paper, we present a method of AR transcriptional repression. The AR is historically a very favorable target in prostate cancer and remains so even when patients develop CRPC.

We have shown biophysical characterization of a transcriptionally important oligonucleotide sequence in the core AR promoter that is consistent with G-quadruplex formation. A BLAST nucleotide alignment search revealed that this sequence is unique to the AR promoter in the human genome and raises the possibility of finding small molecules that may specifically bind to it. Circular dichroism spectra of this sequence was consistent with a parallel structure formation that does not appear to depend on the two central guanine bases. This sequence is extremely G-rich, allowing the possibility of high polymorphism of the G-quadruplex structure. Indirect evidence of these different structural arrangements is seen in the heterogeneity of NMR results where no separate singlets are detectable from the Hoogsteen H-bonds. The relative homogeneity in NMR signal for sequence 3 may be explained by the fewer combinations of stacked guanine quartets or by the presence of a single species. The melting temperature of sequence 3 determined by UV spectroscopy is similar to that

seen for other G-quadruplex promoter quadruplexes that have been targeted by small ligand stabilization^{15,29,30} and raises the possibility that transcriptional repression of the AR may be possible by a similar method.

In order to screen for small molecules that bind and stabilize the AR G-quadruplex, a FRET melting screen was performed. The most promising small ligand, MM45, increased the melting point of the dual labeled sequence 3 oligonucleotide tract by 20.6 K at a concentration of 1 μ M as was shown in Figure 2B. This compares favorably with previous reports evaluating a series of small ligand binding properties with G-quadruplex DNA.³¹ An inactive compound was also identified by FRET melting and used as a negative control in the MTS assay.

Strong evidence is presented that MM45 inhibits AR transcription in prostate cancer cell lines by cell viability assays, an AR promoter driven reporter assay, Western blots, and RT qPCR. IC₅₀ values for MM45 at 72 h by MTS assay for cellular activity were found to lie in the submicromolar range in five different prostate cancer cell lines and one benign prostatic epithelial derived cell line. The negative control, MM10, was found to be far less potent than MM45 and reflects the decreased ability to bind the AR sequence in FRET melting studies. MM45 was also found to be significantly more potent in cell lines that expressed AR, suggesting that AR transcriptional repression may play a role in growth inhibition. Although the difference in IC₅₀ values may be explained by differential uptake of this compound, no such significant difference was detected with the negative control. As most CRPCs continue to express the AR, this is an important finding.⁶

In order to demarcate effects on AR transcription due to changes in cellular activity or other upstream transcription factors, two LNCaP cell lines were cloned with a luciferase reporter assay driven by the core AR promoter. The first cell line included the putative G-quadruplex sequence, whereas this was absent from the control cell line. When compared to the control cell line, luciferase expression of the cell line with the G-

quadruplex sequence was decreased by MM45 in a dose-dependent manner.

AR transcription was also inhibited at the protein and mRNA level in a dose-dependent manner as demonstrated by Western blotting and RT qPCR. mRNA levels for AR target genes are also downregulated. MM45 also affects some of the AR's upstream transcription factors. Effects on Jun, Myc, and Sp1 were quantified, and significant downregulation of Myc and Sp1 was observed, together with upregulation of Jun. Interestingly, these changes all act to repress AR transcription.⁶

We present good evidence that MM45 directly inhibits AR transcription by binding to the AR core promoter G-quadruplex. Further repression of AR transcription may take place via repression of Sp1 and Myc and upregulation of Jun. The precise mechanism by which these upstream transcription factors are modulated has not been investigated in this study but may occur via small molecular interaction with their promoter G-quadruplexes. Myc has a well-characterized G-quadruplex in its promoter that has been previously targeted by small molecular binding.²⁹ Potentially MM45 is also binding here and thus repressing transcription. It is noted that the AR acts as a promoter for Myc transcription and therefore provides a second mechanism of Myc transcriptional repression. Conversely, Jun has a putative G-quadruplex binding site 283bp upstream of its transcription start site,³² where MM45 binding could destabilize formation and promote transcription.

It is likely that MM45 is also acting through other cellular pathways. Current bioinformatic searches estimate that >40% of all genes contain putative G-quadruplex sequences. This AR quadruplex sequence is unusual in that it has a longer loop length than sequences that have been characterized in other oncogenes¹² and may therefore not have been detected by many bioinformatic search algorithms. There is currently no predictive method to determine whether these putative sequences would be stabilized by compounds such as MM45, or whether their stabilization would have any biological significance. The FRET melting experiments revealed that MM45 also stabilized the telomeric control to a similar extent as the AR sequence, and this may represent a further mechanism of growth inhibition.³¹ Other related naphthalene diimide compounds have been previously found to target telomere maintenance in (nonprostate) cancer cell lines.^{29,30}

The repression of AR transcription by stabilization of a quadruplex structure in its promoter represents an alternative treatment pathway for prostate cancer. However, we recognize that it is unlikely that the genomic effects of MM45 are limited to AR transcriptional repression, but are multiple and complex, which may contribute to a therapeutically useful "polytargeting" effect. Further work will be needed to characterize the impact of these possible genome-wide effects in order to determine whether molecules that bind the AR G-quadruplex will be useful therapeutic agents in the fight against prostate cancer.

■ ASSOCIATED CONTENT

■ Supporting Information

Table S1: oligonucleotides used for the biophysical characterization, RT qPCR and PCR amplification; Figures S1 and S2: CD spectra for different cations and CD thermal melting for all four sequences. This material is available free of charge via the Internet at <http://pubs.acs.org>.

■ AUTHOR INFORMATION

Corresponding Author

*E-mail tommitchell@doctors.org.uk; tel +44 7941 626806.

Funding

Work in Cambridge was funded by a grant provided by Addenbrooke's Charitable Trust (Grant No. SD/9618) and a Cancer Research UK project grant (Grant No. C522/A8072). Work in London was funded by a Cancer Research UK program grant (Grant No. C129/A4489). The Balasubramanian Group is supported by a program grant from Cancer Research UK.

Notes

The authors declare no competing financial interest.

■ ACKNOWLEDGMENTS

We gratefully acknowledge Dr. Debbie Sanders and Professor Jason Carroll for helpful advice regarding the investigation of transcriptional regulation.

■ ABBREVIATIONS

AR, androgen receptor; FRET, fluorescence resonance energy transfer; CD, circular dichroism; CRPC, castrate-resistant prostate cancer; IC₅₀, apparent half-maximal inhibitor concentration; NMR, nuclear magnetic resonance; RT qPCR, reverse transcription quantitative polymerase chain reaction; UV spectroscopy, ultraviolet spectroscopy.

■ REFERENCES

- (1) Shen, M. M., and Abate-Shen, C. (2010) Molecular genetics of prostate cancer: new prospects for old challenges. *Genes Dev.* 24, 1967–2000.
- (2) Waltering, K. K., Wallen, M. J., Tammela, T. L., Vessella, R. L., and Visakorpi, T. (2006) Mutation screening of the androgen receptor promoter and untranslated regions in prostate cancer. *Prostate* 66, 1585–1591.
- (3) Scher, H. I., Fizazi, K., Saad, F., Taplin, M. E., Sternberg, C. N., Miller, K., de Wit, R., Mulders, P., Chi, K. N., Shore, N. D., Armstrong, A. J., Flaig, T. W., Flechon, A., Mainwaring, P., Fleming, M., Hainsworth, J. D., Hirmand, M., Selby, B., Seely, L., de Bono, J. S., and Investigators, A. (2012) Increased survival with enzalutamide in prostate cancer after chemotherapy. *N. Engl. J. Med.* 367, 1187–1197.
- (4) de Bono, J. S., Logothetis, C. J., Molina, A., Fizazi, K., North, S., Chu, L., Chi, K. N., Jones, R. J., Goodman, O. B., Jr., Saad, F., Staffurth, J. N., Mainwaring, P., Harland, S., Flaig, T. W., Hutson, T. E., Cheng, T., Patterson, H., Hainsworth, J. D., Ryan, C. J., Sternberg, C. N., Ellard, S. L., Flechon, A., Saleh, M., Scholz, M., Efstathiou, E., Zivi, A., Bianchini, D., Loriot, Y., Chieffo, N., Kheoh, T., Haqq, C. M., and Scher, H. I. (2011) Abiraterone and increased survival in metastatic prostate cancer. *N. Engl. J. Med.* 364, 1995–2005.
- (5) Hu, R., Lu, C., Mostaghel, E. A., Yegnasubramanian, S., Gurel, M., Tannahill, C., Edwards, J., Isaacs, W. B., Nelson, P. S., Bluemn, E., Plymate, S. R., and Luo, J. (2012) Distinct transcriptional programs mediated by the ligand-dependent full-length androgen receptor and its splice variants in castration-resistant prostate cancer. *Cancer Res.* 72, 3457–3462.
- (6) Shiota, M., Yokomizo, A., and Naito, S. (2011) Increased androgen receptor transcription: a cause of castration-resistant prostate cancer and a possible therapeutic target. *J. Mol. Endocrinol.* 47, R25–41.
- (7) Chen, C. D., Welsbie, D. S., Tran, C., Baek, S. H., Chen, R., Vessella, R., Rosenfeld, M. G., and Sawyers, C. L. (2004) Molecular determinants of resistance to antiandrogen therapy. *Nat. Med.* 10, 33–39.
- (8) Snoek, R., Cheng, H., Margiotti, K., Wafa, L. A., Wong, C. A., Wong, E. C., Fazli, L., Nelson, C. C., Gleave, M. E., and Rennie, P. S.

(2009) In vivo knockdown of the androgen receptor results in growth inhibition and regression of well-established, castration-resistant prostate tumors. *Clin. Cancer Res.* 15, 39–47.

(9) Welsbie, D. S., Xu, J., Chen, Y., Borsu, L., Scher, H. I., Rosen, N., and Sawyers, C. L. (2009) Histone deacetylases are required for androgen receptor function in hormone-sensitive and castrate-resistant prostate cancer. *Cancer Res.* 69, 958–966.

(10) Molife, L. R., Attard, G., Fong, P. C., Karavasili, V., Reid, A. H., Patterson, S., Riggs, C. E., Jr., Higano, C., Stadler, W. M., McCulloch, W., Dearnaley, D., Parker, C., and de Bono, J. S. (2010) Phase II, two-stage, single-arm trial of the histone deacetylase inhibitor (HDACi) romidepsin in metastatic castration-resistant prostate cancer (CRPC). *Ann. Oncol.* 21, 109–113.

(11) Sen, D., and Gilbert, W. (1988) Formation of parallel four-stranded complexes by guanine-rich motifs in DNA and its implications for meiosis. *Nature* 334, 364–366.

(12) Balasubramanian, S., Hurley, L. H., and Neidle, S. (2011) Targeting G-quadruplexes in gene promoters: a novel anticancer strategy? *Nat. Rev. Drug Discovery* 10, 261–275.

(13) Siddiqui-Jain, A., Grand, C. L., Bearss, D. J., and Hurley, L. H. (2002) Direct evidence for a G-quadruplex in a promoter region and its targeting with a small molecule to repress c-MYC transcription. *Proc. Natl. Acad. Sci. U. S. A.* 99, 11593–11598.

(14) Fernando, H., Reszka, A. P., Huppert, J., Ladame, S., Rankin, S., Venkitaraman, A. R., Neidle, S., and Balasubramanian, S. (2006) A conserved quadruplex motif located in a transcription activation site of the human c-kit oncogene. *Biochemistry* 45, 7854–7860.

(15) Cogoi, S., and Xodo, L. E. (2006) G-quadruplex formation within the promoter of the KRAS proto-oncogene and its effect on transcription. *Nucleic Acids Res.* 34, 2536–2549.

(16) Drygin, D., Siddiqui-Jain, A., O'Brien, S., Schwaeb, M., Lin, A., Bliesath, J., Ho, C. B., Proffitt, C., Trent, K., Whitten, J. P., Lim, J. K., Von Hoff, D., Anderes, K., and Rice, W. G. (2009) Anticancer activity of CX-3543: a direct inhibitor of rRNA biogenesis. *Cancer Res.* 69, 7653–7661.

(17) Di Antonio, M., Doria, F., Richter, S. N., Bertipaglia, C., Mella, M., Sissi, C., Palumbo, M., and Freccero, M. (2009) Quinone methides tethered to naphthalene diimides as selective G-quadruplex alkylating agents. *J. Am. Chem. Soc.* 131, 13132–13141.

(18) Hampel, S. M., Sidibe, A., Gunaratnam, M., Riou, J. F., and Neidle, S. (2010) Tetrasubstituted naphthalene diimide ligands with selectivity for telomeric G-quadruplexes and cancer cells. *Bioorg. Med. Chem. Lett.* 20, 6459–6463.

(19) Huppert, J. L., and Balasubramanian, S. (2007) G-quadruplexes in promoters throughout the human genome. *Nucleic Acids Res.* 35, 406–413.

(20) Rodriguez, R., Miller, K. M., Forment, J. V., Bradshaw, C. R., Nikan, M., Britton, S., Oelschlaegel, T., Xhemalce, B., Balasubramanian, S., and Jackson, S. P. (2012) Small-molecule-induced DNA damage identifies alternative DNA structures in human genes. *Nat. Chem. Biol.* 8, 301–310.

(21) Faber, P. W., van Rooij, H. C., Schipper, H. J., Brinkmann, A. O., and Trapman, J. (1993) Two different, overlapping pathways of transcription initiation are active on the TATA-less human androgen receptor promoter. The role of Sp1. *J. Biol. Chem.* 268, 9296–9301.

(22) Takane, K. K., and McPhaul, M. J. (1996) Functional analysis of the human androgen receptor promoter. *Mol. Cell. Endocrinol.* 119, 83–93.

(23) Karsisiotis, A. I., Hessari, N. M., Novellino, E., Spada, G. P., Randazzo, A., and Webba da Silva, M. (2011) Topological characterization of nucleic acid G-quadruplexes by UV absorption and circular dichroism. *Angew. Chem., Int. Ed.* 50, 10645–10648.

(24) Adrian, M., Heddi, B., and Phan, A. T. (2012) NMR spectroscopy of G-quadruplexes. *Methods* 57, 11–24.

(25) Mergny, J. L., Phan, A. T., and Lacroix, L. (1998) Following G-quartet formation by UV-spectroscopy. *FEBS Lett.* 435, 74–78.

(26) Rachwal, P. A., and Fox, K. R. (2007) Quadruplex melting. *Methods* 43, 291–301.

(27) Dehm, S. M., and Tindall, D. J. (2006) Ligand-independent androgen receptor activity is activation function-2-independent and resistant to antiandrogens in androgen refractory prostate cancer cells. *J. Biol. Chem.* 281, 27882–27893.

(28) Chlenski, A., Nakashiro, K., Ketels, K. V., Korovaitseva, G. I., and Oyasu, R. (2001) Androgen receptor expression in androgen-independent prostate cancer cell lines. *Prostate* 47, 66–75.

(29) Ambrus, A., Chen, D., Dai, J., Jones, R. A., and Yang, D. (2005) Solution structure of the biologically relevant G-quadruplex element in the human c-MYC promoter. Implications for G-quadruplex stabilization. *Biochemistry* 44, 2048–2058.

(30) Rankin, S., Reszka, A. P., Huppert, J., Zloh, M., Parkinson, G. N., Todd, A. K., Ladame, S., Balasubramanian, S., and Neidle, S. (2005) Putative DNA quadruplex formation within the human c-kit oncogene. *J. Am. Chem. Soc.* 127, 10584–10589.

(31) Muller, S., Sanders, D. A., Di Antonio, M., Matsis, S., Riou, J. F., Rodriguez, R., and Balasubramanian, S. (2012) Pyridostatin analogues promote telomere dysfunction and long-term growth inhibition in human cancer cells. *Org. Biomol. Chem.* 10, 6537–6546.

(32) Hattori, K., Angel, P., Le Beau, M. M., and Karin, M. (1988) Structure and chromosomal localization of the functional intronless human JUN protooncogene. *Proc. Natl. Acad. Sci. U. S. A.* 85, 9148–9152.